IEEE Access
Multidisciplinary | Rapid Review | Open Access Journal

Received November 19, 2020, accepted December 9, 2020, date of publication December 14, 2020,
date of current version December 30, 2020.

Digital Object Identifier 10.1109/ACCESS.2020.3044459

Coupled Planning of Suburban Integrated Energy System With Electric-Biogas-Traffic Considering Fast Charging Station Equalization

CHANGHONG WENG, ZHIJIAN HU, (Member, IEEE), SHIWEI XIE, ZHI CHEN, SHENGHUI LIU, AND YIXING DU
School of Electrical Engineering and Automation, Wuhan University, Wuhan 430072, China
Corresponding author: Zhijian Hu (zhijian_hu@163.com)

This work was supported by the National Natural Science Foundation of China under Grant 51977156.

ABSTRACT Interconnectivity is an important development trend of future energy revolution. A more precise planning model is needed to enhance the interaction of multiple energy sources. In this paper, a joint planning model of active distribution network and transportation network including electricity, gas, heat, and traffic loads is proposed. The main highlights of this model are summarized below. Firstly, this issue puts forward a novel mixed user equilibrium mathematical model nesting fast charging station user equilibrium considering the charging fee, charging time, and queuing time of various charging facilities. Secondly, this work constructs a new generation of suburban integrated energy system (SIES) model considering electricity, biogas, gas, and heat energy, and fully explores the significant role of biogas digestors in a SIES. Thirdly, because the proposed model is a mixed integer nonlinear problem, the piecewise linear method, big-M method, and second-order cone relaxation are used to deal with the nonlinear constraints. Finally, a SIES based on the IEEE 33-node distribution network and a 12-node traffic network is designed for case studies. The results revealed that the new equilibrium will decrease vehicle charging cost strongly up to 19.58%. Moreover, biogas digesters are conducive to new energy consumption, resulting in the proportion of power supply from the upper-level grid falling to 30.87%.

INDEX TERMS Suburban integrated energy system (SIES), planning, user equilibrium, biogas digester.

I. NOMENCLATURE

A. ABBREVIATIONS

SIES	Suburban integrated energy system
FCS-UE	Fast charging station user equilibrium
ADN	Active distribution network
TN	Traffic network
IEH	Integrated energy hub
NGN	Natural gas network
PVT	Photovoltaic thermal
BD	Biogas digestor
B2G	Biogas to gas
EB	Electric boiler
FCF	Fast charging facility
EV	Electric vehicle
NV	Normal vehicle
CV	Charging vehicle

B. SETS

Ω	Sets of all alternative types of a device
Ξ_{od}	Sets of available travel paths for an O-D pair
Ξ_{road}	Sets of roads in traffic network
Θ_{FCS}	Sets of fast charging stations
Θ_{IEH}	Sets of integrated energy hub
$\Theta_{\text{Bus}}/\Theta_{\text{Brch}}$	Sets of buses and branches in the active distribution network
$\Theta_{\text{Brch}}^{\text{from}}/\Theta_{\text{Brch}}^{\text{to}}$	Sets of the first/last nodes of feeders
$[o, d]$	Sets of all O-D pairs

C. VARIABLES

f^{CF}	Charging vehicle flow in FCFs
u^{CF}	The actual cost of FCFs
U^{FCS}	The equivalent equalization cost of FCSs
x	Construction variables
v	Selected variables

The associate editor coordinating the review of this manuscript and approving it for publication was Xiaosong Hu.

$T^{CF}/T^{wait}/T^{charge}$	The actual equivalent time cost of FCFs/queuing/charging
t^{CV}/t^{NV}	The actual total traveling time of CV/NV under current circumstance
T^{CV}/T^{NV}	The equalization cost of CVs/NVs
$f^{road}/f^{CV}/f^{NV}$	The total/CV/NV flow on traffic roads
$T^{in}/T^{W}/T^{out}$	The internal/wall/external temperature of biogas digestors
N	Construction quantity
$\tilde{P}/\tilde{Q}/\tilde{h}$	Adjusted active/reactive/heat power
λ^{c}/λ^{d}	Charging power/discharging power
χ^{c}/χ^{d}	Charging/discharging indicator indexes
S^{SOC}	State of charge

D. PARAMETERS

fd	Traffic demands
T_0^{bio}	The best reaction temperature of biogas digester
C^{in}/C^{W}	Thermal insulation parameters of biogas digesters
R^{in}/R^{W}	Thermal consumption parameters of biogas digesters
β_{min}/β_{max}	The minimum/maximum curtail percentage
$P/Q/h/g$	Original active/reactive/heat/gas power
η	Conversion efficiency
$PD/QD/gD/hD$	Active/reactive/gas/heat demands
R_{ij}/X_{ij}	Feeder resistance/reactance
$\bar{P}^{line}/\bar{Q}^{line}$	Upper limit of active/reactive power of feeder
$\underline{\hat{U}}/\bar{\hat{U}}$	Lower/upper limit of nodes voltage
$\underline{P}^{gen}/\bar{P}^{gen}$	The minimum/maximum active power of upper-level grid
$\underline{Q}^{gen}/\bar{Q}^{gen}$	The minimum/maximum reactive power of upper-level grid
c	Single equipment cost
N_{max}	Maximum investment amount

II. INTRODUCTION

Nowadays, great changes are taking place in energy pattern of the world. The trend of energy diversification facilitates all components being closely linked to maximize energy utilization [1]. Against this background, integrated energy system (IES) combining independent systems of various energy forms has emerged [2]. IES is equipped with energy coupling components, such as combined heat and power (CHP) and power to gas (P2G), to manage and transform each energy flow, which breaks the traditional barriers that different systems can only be planned independently. As a result, higher power supply reliability, lower cost and better power quality can be achieved [3]. Up to now, many governments and enterprises have put forward research projects and engineering practices on the IES, such as ''New Infrastructure'' raised by State Grid in China [4], the ''Japan smart community alliance'' in Japan [5], ''GRID 2030'' in the United States [6].

In view of the benefits of IES, the research on the expansion planning of IES has attracted more and more attention in recent years. A new multi-energy system planning model starting with nothing was proposed in [7]. In this model, integrated energy hub (IEH) was regarded as a directed acyclic graph with multiple layers which was an innovative application of graph theory, and then planned in two steps divided into investment and operation. In [8], deep research applied to planning problem of coupled active distribution network (ADN) and natural gas network (NGN) has been done. The planning results demonstrated that it was beneficial for IES to take active managements such as terminal voltage adjustment, reactive power compensation and energy storage device management. Literature [9] proposed a two-layer multi-stage model to plan the IES coupled with electric distributed network and NGN, whose upper layer used the improved binary particle swarm optimization to determine the location and capacity of target system, while its lower layer used the internal point method to decide the optimal operation mode in several stages. In [10], the two-level planning model aiming at levelized cost took hydrogen energy into consideration in the IES. Besides, a reconstruction decomposition algorithm was proposed to solve the model. In [11], a long-tern coordinated expansion model was designed to solve the multi-stage planning problem of multi-energy system coupling gas, heat, and electric systems. In addition to the traditional IES that considers electricity and natural gas together mentioned in the above references, biogas, as one of the important renewable energy sources with low cost and easy production, has also attracted the attention of scholars in this field. In [12], a planning task, containing a biological biogas digestor model, was conducted for independent microgrid systems in remote areas that have poor construction of ADN. There was a research paper showing that biogas digestor with electric-heat feedback can improve biogas production performance and ensure that it can meet the gas demand of users economically in a low temperature environment [13]. Further study, [14] discussed the optimal dispatching strategies of multiple such microgrids that allow energy exchange through the trading market. However, there still is no a planning model for ADNs with integrated energy stations while considering biogas energy.

Not only IESs but also electric vehicles (EVs) have drawn society focusing because of its environmental friendliness. With the growth of EV ownership, the charging risks continue to increase, which has brought challenges to the safe operation of ADN [15]. In line with this tendency, it's essential to considered EVs' charging load into initial planning stage. A planning for fast charging station (FCS) using a new graph computing method was done in [15], but this article used flow capture model to estimate the charging load, which leads to ignoring the impact of charging stations' location on the users' travel path. In [16], authors discussed several different

modes of charging load regulation and control, showing that orderly charging and discharging management plays a positive role in safe and economic operation of ADN, but ignored the spatial transfer characteristics of EV charging load. [17] comprehensively considered travel path, charging opportunity and marginal price factors of EV users to pursue the optimal operation state of ADN and TN. Inspired by [17], an IES planning model innovatively coupling three networks, i.e. ADN, TN, and NGN, at the same time were proposed in [18]. What's more, in the simulation of EV users' travel behavior, the model also takes into charging waiting time as an index, but omitted users' selection behavior of different types of charging facilities. The same team has other explorations in FCS planning, that is, in [19], they proposed a three-dimensional function linearization method of travel time on road capacity growth, and explored the impact of road expansion on traffic load.

To the best of our knowledge, there still remains research gaps from the following aspects:

1) The studies on the planning of an IES coupled with IEH, TN and ADN are still in their infancy. More than that, most of current studies consider the NGN as main gas source to meet users' demands [7]–[9], which give rise to the influences of users' gas demand and EV charging flow on IES planning in suburban areas or somewhere without mature NGN are ignored.

2) Although there are relatively complete studies on the charging rules of EVs, no relevant reports have been found to consider the influence of internal structure of FCSs on users' charging behaviors, thus affecting the planning results.

Based on the aforementioned discussions, a coupling planning model for suburban integrated energy system with ADN, TN, and IEH is proposed in this paper to fill the research gap. In ADN, the main planning items are the constructions of line upgrading, distributed generations (DGs) and electricity storages (ESs), and at the same time, simple active managements are carried out such as static var compensator (SVC) investment, DG curtailment and demand response (DR). In IEH, a new model including BDs, biogas to gas (B2Gs), gas boilers (GBs), electric boilers (EBs), combined heat and power (CHPs), power to gas (P2Gs), heat storages (HSs), and gas storages (GSs) is proposed, and it's worth mentioning that BD model contains thermal feedback mechanism whose gas production superiority has been proven [13]. In TN, a novel mixed user equilibrium based on Wardrop theory is applied to simulate steady traffic flow, and furthermore, FCS user equilibrium (FCS-UE) is developed to simulate the actions of users' selection of different fast charging facility (FCF) types, affected by queuing time, charging time, and charging fee mainly. Reviewing the above, it can be inferred that the proposed model is a large mixed integer nonlinear problem (MINLP). To obtain accurate planning results efficiently, the piecewise linearization method (PWL), big-M method, and second-order cones relaxation (SOCR) are utilized in relaxing model. At last, the effectiveness and advance of the proposed model are tested by the IEEE 33-node distributed network, a 12-node transportation network, and three new IEHs coupled together.

The contribution of this paper to fill the research gap can be summarized as follows:

1) A novel mixed user equilibrium model nesting FCS-UE is proposed. Under the background of information sharing, this new equilibrium can simulate steady-state traffic flow in the whole process of user travel and charging, and realize refined planning modeling in FCSs.

2) A new IEH model containing biogas digestors and fast charging stations is proposed. Moreover, it's the first time to develop a SIES planning model with electric, heat, gas, biogas, traffic energy flow and embedded in ADN and TN.

The remain sections of this paper are organized as follow. Section II introduces the SIES instruction. Then, the novel mixed user equilibrium nesting fast charging station user equilibrium and its planning expansion model are developed in Section III. Section IV demonstrates the SIES modeling and Section V illustrates the linear mathematical planning model of SIES. Next, the proposed system is tested and numerical results are analyzed in Section VI. Finally, conclusions are summarized in Section VII.

III. NEW GENERATION SUBURBAN INTEGRATED ENERGY SYSTEM (SIES) ARCHITECTURE

Land resources within urban are increasingly scarce, more and more people are migrating to the edge of city, and IEH with a certain scale is bound to move to suburbs for relieving pressure on urban land use. Against this background, this paper produces a new generation SIES model, which conforms to the trend of expanding EV users and takes the fact that there is no mature NGN coverage in suburbs into account. As the system structure diagram shown in Fig.1, the components of SIES are partitioned into three parts, that are (a) IEH: renewable generation supplies (wind generators (WGs), photovoltaic thermals (PVTs), and BDs), energy conversion devices (B2Gs, P2Gs, CHPs, GBs, EBs, and FCFs) and energy storage devices (ESs, GSs, and HSs), (b) energy demand: traffic load, power load, gas load, and heat load, (c) extra network: the ADN and the TN. It is worth mentioning that thanks to the continuous development of communication technology, the interaction of various energy sources is closer and more immediate. The specific performances are: EV users can optimize the charging plan under traffic guidance measures and provide it to the SIES equipment decision; conversely, SIES can affect the actual equilibrium of TN by configuring different numbers and types of FCFs. ADN and TN are connected through IEH to form an interdependent and interact SIES.

IV. TRANSPORTATION NETWORK MODELING WITH THE NOVEL USER EQUILIBRIUM

A. FCS USER EQUILIBRIUM

1) DEFINITION AND PLANNING EXPANSION EQUILIBRIUM

The actual operation of FCSs has a relatively large impact on the steady-state vehicle flow distribution of the TN, especially

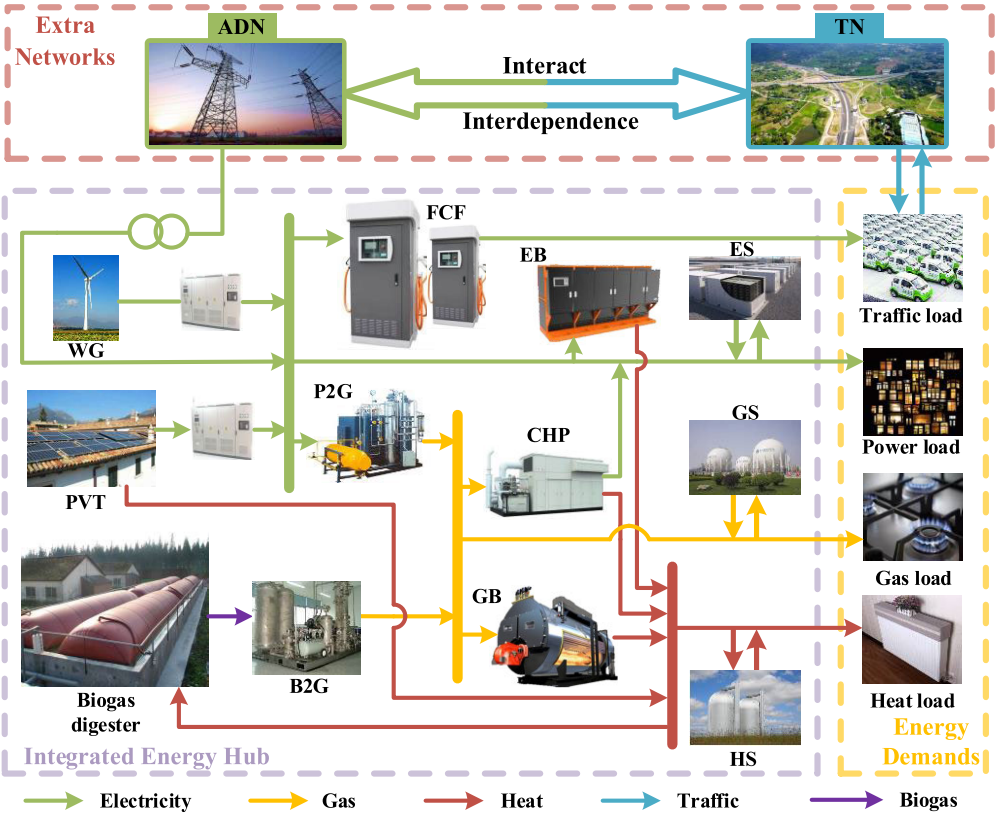

FIGURE 1. The structure of suburban integrated energy system proposed in this article.

on the route selection of users with charging needs. Therefore, this paper proposes the concept of FCS user equilibrium, and analyzes the steady-state operation of FCSs. Its specific physical definition is as follows:

Definition: EV users arriving at a certain FCS will always choose the appropriate FCFs according to queuing time, charging time, charging cost, and selected equipment must be the best choice in current state (that is, the lowest cost). Based on this objective selection mode, in a steady state, the cost of choosing different types of FCFs in a FCS is the same, and any user who changes the current selection will pay higher cost. This steady state is defined as FCS user equilibrium (FCS-UE).

Then the mathematical expression form of FCS-UE is given below:

$$\begin{cases} f_{k,t}^{\mathrm{CF}}(u_{k,t}^{\mathrm{CF}} - U_t^{\mathrm{FCS}}) = 0 \\ f_{k,t}^{\mathrm{CF}} \geq 0 \\ u_{k,t}^{\mathrm{CF}} - U_t^{\mathrm{FCS}} \geq 0 \\ k \in \Omega_{\mathrm{CF}}, \forall t \end{cases} \tag{1}$$

In (1), the first equation constraints users' selection mode; the second constraint restricts charging flow range; the third represents the cost object request. Since this paper discusses SIES planning problem including FCSs, the construction of FCFs should be considered into FCS-UE. Logic variable x_k^{CF} is introduced to imply the construction condition of each FCF and binary variable $v_{k,t}^{\mathrm{CF}}$ is to denote users' selections. Then, the planning expansion equilibrium of FCS-UE is expressed as the following disjunctive equation:

$$\begin{array}{ccccc} \text{Situation 1} & & & \text{Situation 2} & \text{Situation 3} \\ \left[\begin{array}{l} \forall x_k^{\mathrm{CF}} = 1 \\ v_{k,t}^{\mathrm{CF}} = 1 \\ f_{k,t}^{\mathrm{CF}} > 0 \\ u_{k,t}^{\mathrm{CF}} = U_t^{\mathrm{CF}} \end{array}\right. & \left|\begin{array}{l} v_{k,t}^{\mathrm{CF}} = 0 \\ f_{k,t}^{\mathrm{CF}} = 0 \\ u_{k,t}^{\mathrm{CF}} \geq U_t^{\mathrm{CF}} \end{array}\right. & \vee & \left[\begin{array}{l} \exists x_k^{\mathrm{CF}} = 0 \\ v_{k,t}^{\mathrm{CF}} = 0 \\ f_{k,t}^{\mathrm{CF}} = 0 \\ u_{k,t}^{\mathrm{CF}} \in \mathbb{R} \end{array}\right. & \vee & \left[\begin{array}{l} \forall x_k^{\mathrm{CF}} = 0 \\ v_{k,t}^{\mathrm{CF}} = 0 \\ f_{k,t}^{\mathrm{CF}} = 0 \\ u_{k,t}^{\mathrm{CF}} = U_{\max}^{\mathrm{CF}} \end{array}\right. \end{array}$$
$$x_k^{\mathrm{CF}} \in \{0,1\}, \quad v_{k,t}^{\mathrm{CF}} \in \{0,1\}, \ k \in \Omega_{\mathrm{CF}}, \ \forall t \tag{2}$$

There are three different situations of FCS-UE changing with the configuration of FCFs, that are all construction (Situation 1), partial construction (Situation 2) and no construction (Situation 3). In Situation 1, all types of FCFs are requested to satisfy FCS-UE. If $v_{k,t}^{\mathrm{CF}}$ is true, $f_{k,t}^{\mathrm{CF}} > 0$ and $u_{k,t}^{\mathrm{CF}} = U_t^{\mathrm{CF}}$ are valid; otherwise, $f_{k,t}^{\mathrm{CF}} = 0$ and $u_{k,t}^{\mathrm{CF}} > U_t^{\mathrm{CF}}$. In situation 2, some types of FCFs aren't equipped which don't participate in the equilibrium. Correspondingly, if $x_k^{\mathrm{CF}} = 0$, no EV user can select this type of FCFs for charging. And in order to avoid the influence of the special circumstance on original equilibrium, theoretical use cost is not restricted by the equilibrium and can be any real value. In situation 3, no FCF is built, so there is no FCS-UE. As a result, the balanced cost ought to be set an extremely bad

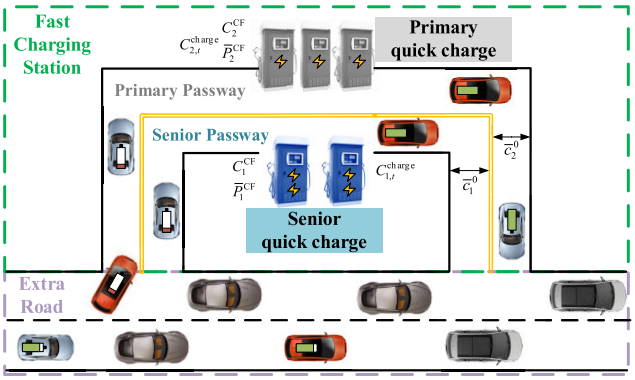

FIGURE 2. Schematic diagram of fast charging station.

value $U_{\max}^{\mathrm{CF}}$ to eliminate impact on travel path choice of EV in TN. But (2) is non-convex, which is not conducive to solution of FCS-UE, so this paper uses big-M method [20] to relax, thus yielding:

$$v_{k,t}^{\mathrm{CF}} \le x_k^{\mathrm{CF}} \tag{3}$$

$$0 \le f_{k,t}^{\mathrm{CF}} \le \mathrm{M} * v_{k,t}^{\mathrm{CF}} \tag{4}$$

$$-\mathrm{M} * (1 - x_k^{\mathrm{CF}}) \le u_{k,t}^{\mathrm{CF}} - U_t^{\mathrm{CF}} \le \mathrm{M} * (1 - v_{k,t}^{\mathrm{CF}}) \tag{5}$$

$$0 \le U_{\max}^{\mathrm{CF}} - u_{k,t}^{\mathrm{CF}} \le \mathrm{M} * \sum_{k \in \Omega_{\mathrm{CF}}} x_k^{\mathrm{CF}} \tag{6}$$

where M is a big constant. (3) implies FCF investment is a sufficient condition for selection. (4) expresses the utility of logic choice variables, which constrain the available range of charging flow. (5) is the key formula of FCS-UE as well as the accurate expression of the restricted equivalent cost under various situations. And the equilibrium time in the extreme case of no construction is represented by (6). After conversion, FCS-UE expression is transformed into convex which is useful in SIES planning.

2) TIME AND COST SPENT IN FCSs

Conventionally, EV users who want to get recharged need to go through two steps: queuing and charging, as demonstrated in the schematic diagram of the FCS (Fig. 2). Meanwhile, the cost paid by users is not only economic costs (charging fees), but also time costs (queuing time and charging time). Therefore, the equivalent time cost function of FCSs can be calculated as:

$$T_{k,t}^{\mathrm{CF}} = T_{k,t}^{\mathrm{wait}} + T_k^{\mathrm{charge}} + C_k^{\mathrm{charge}}/\varsigma = u_{k,t}^{\mathrm{CF}} \tag{7}$$

$$T_{k,t}^{\mathrm{wait}} = t_k^0 \cdot J_C \cdot \frac{f_{k,t}^{\mathrm{CF}}}{\bar{c}_k^0 - f_{k,t}^{\mathrm{CF}}} \tag{8}$$

$$T_k^{\mathrm{charge}} = t_k^0 \tag{9}$$

where ς is the cost-time conversion factor. In line with [17] and [18], this paper employs Davidson function [21] based on queuing theory to characterize the queuing time in FCSs as (8) shown, where, t_k^0 is the service time, which is numerically equal to $T_{k,t}^{\mathrm{charge}}$ as (9) displayed; J_C is defined as the time shape coefficient of Davidson function and $\bar{c}_k^0$ characterizes the maximum service capacity of FCS road. It's noted that all time units in (7)-(9) are minute.

3) CHARGING FLOW

In terms of the relationship between supplies and demands, the feasible range of charging flow is defined as:

$$\begin{aligned} \sum_k f_{k,t,w}^{\mathrm{CF}} &= f_{w,t}^{\mathrm{CV}} \\ f_{k,t,w}^{\mathrm{CF}} &\ge 0 \\ k \in \Omega_{\mathrm{CF}}, \quad w &\in \Theta_{\mathrm{FCS}} \end{aligned} \tag{10}$$

B. A MIXED USER EQUILIBRIUM MODEL OF TN NESTING FCS-UE

1) MATHEMATICAL EXPRESSION OF THE MIXED USER EQUILIBRIUM

In actual TNs, we use whether the vehicle needs to be charged as a criterion, and divide it into two types: charging vehicles (CVs) and normal vehicles (NVs). Their respective travel paths are different. The travel route chosen by the former must be able to complete the travel tasks and need to pass through a FCS, while the latter choose all routes that can reach the destination. In light of such a travel law, taking origin-destination (O-D) pairs to express travel needs, Wardrop user principle [22] is exploited to establish mixed user equilibrium model of TN:

$$\text{CV equilibrium} \begin{cases} f_{od,n,t}^{\mathrm{CV}}(t_{od,n,t}^{\mathrm{CV}} - T_{od,t}^{\mathrm{CV}}) = 0 \\ f_{od,n,t}^{\mathrm{CV}} \ge 0 \\ t_{od,n,t}^{\mathrm{CV}} - T_{od,t}^{\mathrm{CV}} \ge 0 \\ \forall [o,d], n \in \Xi_{od}^{\mathrm{CV}}, \forall t \end{cases} \tag{11}$$

$$\text{NV equilibrium} \begin{cases} f_{od,n,t}^{\mathrm{NV}}(t_{od,n,t}^{\mathrm{NV}} - T_{od,t}^{\mathrm{NV}}) = 0 \\ f_{od,n,t}^{\mathrm{NV}} \ge 0 \\ t_{od,n,t}^{\mathrm{NV}} - T_{od,t}^{\mathrm{NV}} \ge 0 \\ \forall [o,d], n \in \Xi_{od}^{\mathrm{NV}}, \forall t \end{cases} \tag{12}$$

Logic variables $v_{od,n,t}^{\mathrm{CV}}$ and $v_{od,n,t}^{\mathrm{NV}}$ are introduced to transform nonlinear expression into convex expressions using big-M method:

$$\text{CV equilibrium} \begin{cases} 0 \le f_{od,n,t}^{\mathrm{CV}} \le \mathrm{M} \cdot v_{od,n,t}^{\mathrm{CV}} \\ 0 \le t_{od,n,t}^{\mathrm{CV}} - T_{od,t}^{\mathrm{CV}} \le \mathrm{M} \cdot (1 - v_{od,n,t}^{\mathrm{CV}}) \\ v_{od,n,t}^{\mathrm{CV}} \in \{0,1\}, \ \forall [o,d], n \in \Xi_{od}^{\mathrm{CV}}, \forall t \end{cases} \tag{13}$$

$$\text{NV equilibrium} \begin{cases} 0 \le f_{od,n,t}^{\mathrm{NV}} \le \mathrm{M} \cdot v_{od,n,t}^{\mathrm{NV}} \\ 0 \le t_{od,n,t}^{\mathrm{NV}} - T_{od,t}^{\mathrm{NV}} \le \mathrm{M} \cdot (1 - v_{od,n,t}^{\mathrm{NV}}) \\ v_{od,n,t}^{\mathrm{NV}} \in \{0,1\}, \ \forall [o,d], n \in \Xi_{od}^{\mathrm{NV}}, \forall t \end{cases} \tag{14}$$

The new constraints (13)-(14) show that the travel costs of routes are not higher than the equilibrium cost is a necessary and sufficient condition for choosing these routes, which is in full compliance with the physical meaning of Wardrop user equilibrium.

2) TRAVEL TIME AND COST

Similarly, discuss CV and NV separately.

$$t_{od,n,t}^{\mathrm{CV}} = T_{od,n,t}^{\mathrm{Traveling}} + U_{w,t}^{\mathrm{FCS}} \quad \forall[o,d],\ n \in \Xi_{od}^{\mathrm{CV}},\ \forall t,\quad w \in \Theta_{\mathrm{FCS}} \cap \Xi_{od}^{\mathrm{CV}} \tag{15}$$

$$t_{od,n,t}^{\mathrm{NV}} = T_{od,n,t}^{\mathrm{Traveling}} \quad \forall[o,d],\ n \in \Xi_{od}^{\mathrm{NV}},\ \forall t \tag{16}$$

$$T_{od,n,t}^{\mathrm{Traveling}} = \sum_{r} T_{r,t}^{\mathrm{BPR}} \quad \forall[o,d],\ n \in \Xi_{od},\ r \in n,\ \forall t \tag{17}$$

$$T_{r,t}^{\mathrm{BPR}} = t_r^0 \left[1 + 0.15 \times \left(\frac{f_{r,t}^{\mathrm{road}}}{c_r^0}\right)^4\right] \quad r \in \Xi_{\mathrm{road}},\quad \forall t \tag{18}$$

where, $\Theta_{\mathrm{FCS}} \cap \Xi_{od}^{\mathrm{CV}}$ denotes the set of FCSs in CV route and $r \in n$ means r is the road section traveled by plan n. As (15) illustrated, the total travel time of CV includes road travel time and FCS equivalent time cost; while NV has no charging action, so it only involves the former, according to (16). Equation (17) is the concrete expression of users' road travel time, which is the cumulative travel time of each road. In (18), Bureau of Public Road (BPR) function [23] is drawn on to characterize road travel time.

3) MIXED TRAFFIC FLOW

For such a traffic mixed equilibrium system, it involves the overlap of double traffic flows. The quantitative relationship of mixed traffic flow in TN is expressed as:

$$f_{r,t}^{\mathrm{road}} = \sum_{n} f_{n,t}^{\mathrm{CV}} + \sum_{n} f_{n,t}^{\mathrm{NV}} \quad r \in n,\ \forall t \tag{19}$$

$$\begin{cases} \sum_{n} f_{n,t}^{\mathrm{CV}} = f d_{od,t}^{\mathrm{CV}} \\ f_{n,t}^{\mathrm{CV}} \geq 0 \end{cases} \quad \forall[o,d],\quad n \in \Xi_{od},\ \forall t \tag{20}$$

$$\begin{cases} \sum_{n} f_{n,t}^{\mathrm{NV}} = f d_{od,t}^{\mathrm{NV}} \\ f_{n,t}^{\mathrm{NV}} \geq 0 \end{cases} \quad \forall[o,d],\quad n \in \Xi_{od},\ \forall t \tag{21}$$

Equation (19) shows the superposition of two components of steady-state traffic flow on roads, namely the flows of CV and NV. The demand conservation equations between O-D pairs of CV and NV in TN are defined in (20)-(21).

V. SUBURBAN INTEGRATED ENERGY SYSTEM MODELING

A. INTEGRATED ENERGY HUB MODELING

1) BIOGAS DIGESTER

The BD is essentially a renewable source. Due to low emission and widespread distribution of biomass, it has been used widely in the word especially in suburban areas where raw materials are abundant. The working mechanism of BDs is organic matters such as manure, weeds, and straw are decomposed by anaerobic bacteria, and a large amount of biogas is produced during the period. Furthermore, study has shown

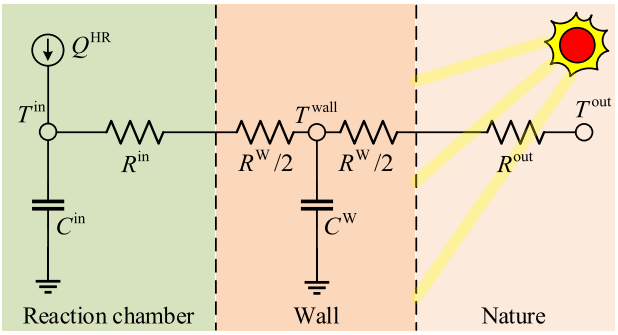

FIGURE 3. The heat conduction model of BD with thermal feedback mechanism.

that in mid-temperature anaerobic decomposition process, the biggest environmental factor affecting the efficiency is the reaction temperature [24], that indicates too high or too low temperature is not conducive to survival of anaerobic bacteria. In [13], the basic regular expression of gas production and reaction temperature of the BD is obtained by fitting data, which is simplified as:

$$g^{\mathrm{bio}} = a\left|T^{\mathrm{in}} - T_0^{\mathrm{bio}}\right| + b \tag{22}$$

where, a and b are fitting parameters, and $a < 0$. (22) is in line with the basic trend that when reaction tank temperature is closer to the optimal reaction temperature, biogas production is more sufficient. Summarized by survival law of anaerobic bacteria, $T_0^{\mathrm{bio}} = 35°\mathrm{C}$.

As a place for anaerobic decomposition, BDs' thermodynamic characteristics should be focus of our attention. Based on the thermodynamic conduction model established in [25], in this paper, the temperature attenuation effect is equivalent to thermal resistance, and the insulation effect is equivalent to heat capacity. The heat conduction model of the BD with thermal feedback mechanism is shown in Fig. 3. And heat conduction equation is:

$$\frac{T_t^{\mathrm{W}} - T_t^{\mathrm{in}}}{R^{\mathrm{in}} + R^{\mathrm{W}}/2} + Q_t^{\mathrm{HR}} = C^{\mathrm{in}} \frac{T_t^{\mathrm{in}} - T_{t-1}^{\mathrm{in}}}{\Delta t} \tag{23}$$

$$\frac{T_t^{\mathrm{out}} - T_t^{\mathrm{W}}}{R^{\mathrm{out}} + R^{\mathrm{W}}/2} + \frac{T_t^{\mathrm{in}} - T_t^{\mathrm{W}}}{R^{\mathrm{in}} + R^{\mathrm{W}}/2} = C^{\mathrm{W}} \frac{T_t^{\mathrm{W}} - T_{t-1}^{\mathrm{W}}}{\Delta t} \tag{24}$$

where Q_t^{HR} represents feedback heat. In (23), the inside of the BD is the object of heat conduction, and (24) aims at the wall.

2) WIND GENERATION

$$(1 - \beta_{\max}^{\mathrm{WG}})\widehat{P}_{w,t}^{\mathrm{WG}} \leq P_{w,t}^{\mathrm{WG}} \leq \widehat{P}_{w,t}^{\mathrm{WG}} \tag{25}$$

$$-P_{w,t}^{\mathrm{WG}} \cdot \tan(\arccos(\theta_{\max}^{\mathrm{WG}})) \leq Q_{w,t}^{\mathrm{WG}} \leq P_{w,t}^{\mathrm{WG}} \cdot \tan(\arccos(\theta_{\max}^{\mathrm{WG}})) \tag{26}$$

$$0 \leq \widehat{P}_{w,t}^{\mathrm{WG}} \leq \sum_{k} N_{w,k}^{\mathrm{WG}} \bar{P}_{k}^{\mathrm{WG}} \tag{27}$$

$$k \in \Omega_{\mathrm{WG}},\quad w \in \Theta_{\mathrm{IEH}},\ \forall t$$

3) PHOTOVOLTAIC THERMAL

$$(1-\beta_{\max}^{\mathrm{PVT}})\widehat{P}_{w,t}^{\mathrm{PVT}} \le P_{w,t}^{\mathrm{PVT}} \le \widehat{P}_{w,t}^{\mathrm{PVT}} \tag{28}$$

$$-P_{w,t}^{\mathrm{PVT}}\cdot\tan(\arccos(\theta_{\max}^{\mathrm{PVT}})) \le Q_{w,t}^{\mathrm{PVT}} \le P_{w,t}^{\mathrm{PVT}}\cdot\tan(\arccos(\theta_{\max}^{\mathrm{PVT}})) \tag{29}$$

$$h_{w,t}^{\mathrm{PVT}} = \widehat{h}_{w,t}^{\mathrm{PVT}} \tag{30}$$

$$0 \le \widehat{P}_{w,t}^{\mathrm{PVT}} \le \sum_k N_{w,k}^{\mathrm{PVT}}\bar{P}_k^{\mathrm{PVT}} \tag{31}$$

$$0 \le \widehat{h}_{w,t}^{\mathrm{PVT}} \le \sum_k N_{w,k}^{\mathrm{PVT}}\bar{h}_k^{\mathrm{PVT}} \tag{32}$$

$$k \in \Omega_{\mathrm{PVT}}, \quad w \in \Theta_{\mathrm{IEH}}, \ \forall t$$

Similar active management measures are adopted in WGs and PVTs. Equations (25) and (28) perform wind and solar abandonments respectively, while heat abandonment is not considered as (30) shown. In (26) and (29), reactive power output range is restricted in form of ultimate power factor. (27), (31), and (32) indicate that maximum output power is proportional to the number of WGs and PVTs installed.

4) POWER TO GAS

$$g_{w,t}^{\mathrm{P2G}} = \frac{3.412\eta_{\mathrm{P2G}}\cdot P_{w,t}^{\mathrm{P2G}}}{\mathrm{GHV}} \tag{33}$$

$$0 \le P_{w,t}^{\mathrm{P2G}} \le \sum_k N_{w,k}^{\mathrm{P2G}}\bar{P}_k^{\mathrm{P2G}} \tag{34}$$

$$k \in \Omega_{\mathrm{P2G}}, \quad w \in \Theta_{\mathrm{IEH}}, \ \forall t$$

5) COMBINED HEAT AND POWER

$$P_{w,t}^{\mathrm{CHP}} = \frac{\mathrm{GHV}\cdot\eta_{\mathrm{CHP}}^{\mathrm{e}}\cdot g_{w,t}^{\mathrm{CHP}}}{3.412} \tag{35}$$

$$h_{w,t}^{\mathrm{CHP}} = \frac{\mathrm{GHV}\cdot\eta_{\mathrm{CHP}}^{h}\cdot g_{w,t}^{\mathrm{CHP}}}{3.412} \tag{36}$$

$$0 \le g_{w,t}^{\mathrm{CHP}} \le \sum_k N_{w,k}^{\mathrm{CHP}}\bar{g}_k^{\mathrm{CHP}} \tag{37}$$

$$k \in \Omega_{\mathrm{CHP}}, \quad w \in \Theta_{\mathrm{IEH}}, \ \forall t$$

6) GAS BOILER

$$h_{w,t}^{\mathrm{GB}} = \frac{\mathrm{GHV}\cdot\eta_{\mathrm{GB}}\cdot g_{w,t}^{\mathrm{GB}}}{3.412} \tag{38}$$

$$0 \le g_{w,t}^{\mathrm{GB}} \le \sum_k N_{w,k}^{\mathrm{GB}}\bar{g}_k^{\mathrm{GB}} \tag{39}$$

$$k \in \Omega_{\mathrm{GB}}, \quad w \in \Theta_{\mathrm{IEH}}, \ \forall t$$

7) ELECTRIC BOILER

$$h_{w,t}^{\mathrm{EB}} = \eta_{\mathrm{EB}}\cdot P_{w,t}^{\mathrm{EB}} \tag{40}$$

$$0 \le P_{w,t}^{\mathrm{EB}} \le \sum_k N_{w,k}^{\mathrm{EB}}\bar{P}_k^{\mathrm{EB}} \tag{41}$$

$$k \in \Omega_{\mathrm{EB}}, \quad w \in \Theta_{\mathrm{IEH}}, \ \forall t$$

8) FAST CHARGING FACILITY

$$0 \le f_{w,k,t}^{\mathrm{CF}} < \bar{c}_k^0 \tag{42}$$

$$P_{w,t}^{\mathrm{EV}} = \upsilon_{\mathrm{Tr}}\cdot f_{w,t}^{\mathrm{CV}} \le N_{w,k}^{\mathrm{CF}}\bar{P}_k^{\mathrm{CF}} \tag{43}$$

$$0 \le N_{w,k}^{\mathrm{CF}} \le \mathrm{M}\cdot x_{w,k}^{\mathrm{CF}} \tag{44}$$

$$k \in \Omega_{\mathrm{CF}}, \quad w \in \Theta_{\mathrm{IEH}}, \ \forall t$$

9) BIOGAS TO GAS

$$g_{w,t}^{\mathrm{gas}} = \eta_{\mathrm{B2G}}g_{w,t}^{\mathrm{B2G}} \tag{45}$$

$$0 \le g_{w,t}^{\mathrm{B2G}} \le N_w^{\mathrm{B2G}}\bar{g}^{\mathrm{B2G}} \tag{46}$$

$$w \in \Theta_{\mathrm{IEH}}, \quad \forall t$$

Equations (33)-(46) establish energy conversion supply modellings of IEH, where 3.412 is unit conversion coefficient (1w = 3.412 btu/h) and gross heating value satisfies GHV = 4.0611×10^4btu/m^3 normally. Notably, the flow of CVs at each FCS is limited by the maximum capacity of road at corresponding station in (42). And (43) indicates charging power demands are positively related to charging flow, where υ_{Tr} is unit share. Besides, the number of FCFs is constrained by FCS construction intention, as shown in (44). (45) gives the conversion relationship from biogas to natural gas, the physical basis for that is both main components are methane.

10) ELECTRIC/GAS/HEAT STORAGE

$$0 \le \lambda_{w,t}^{\mathrm{c}} \le \mathrm{M}\cdot\chi_{w,t}^{\mathrm{c}} \tag{47}$$

$$0 \le \lambda_{w,t}^{\mathrm{d}} \le \mathrm{M}\cdot\chi_{w,t}^{\mathrm{d}} \tag{48}$$

$$\chi_{w,t}^{\mathrm{c}} + \chi_{w,t}^{\mathrm{d}} \le 1 \tag{49}$$

$$\chi_{w,t}^{\mathrm{c}} \in \{0,1\}, \quad \chi_{w,t}^{\mathrm{d}} \in \{0,1\}$$

$$0 \le \lambda_{w,t}^{\mathrm{c}} \le \sum_k N_{w,k}^{\mathrm{S}}\bar{\lambda}_k^{\mathrm{c}} \tag{50}$$

$$0 \le \lambda_{w,t}^{\mathrm{d}} \le \sum_k N_{w,k}^{\mathrm{S}}\bar{\lambda}_k^{\mathrm{d}} \tag{51}$$

$$0 \le S_{w,t}^{\mathrm{SOC}} \le \sum_k N_{w,k}^{\mathrm{S}}\bar{S}_{w,t}^{\mathrm{S}} \tag{52}$$

$$\sum_t \lambda_{w,t}^{\mathrm{c}} + \sum_t \lambda_{w,t}^{\mathrm{d}} = 0 \tag{53}$$

$$S_{w,t}^{\mathrm{S}} = S_{w,t-1}^{\mathrm{S}} + (\eta_{\mathrm{S}}^{\mathrm{c}}\lambda_{w,t}^{\mathrm{c}} - \lambda_{w,t}^{\mathrm{d}}/\eta_{\mathrm{S}}^{\mathrm{d}})\Delta t \tag{54}$$

$$k \in \{\Omega_{\mathrm{ES}}/\Omega_{\mathrm{GS}}/\Omega_{\mathrm{HS}}\}, \quad w \in \Theta_{\mathrm{IEH}}, \ \forall t$$

The charging and discharging characteristics of energy conversion devices are collectively expressed in (47)-(54). Binary variables χ^{c} and χ^{d} are introduced to characteristic the mutual exclusion of charge and discharge assisted by big-M method, as reported in (47)-(49). Equations (50)-(51) constrained the maximum power, then the max capacity is limited in (52). In (53), the charge is request to be equal to discharge during planning period ensuring the recyclability. At last, changing law of the capacity at each moment is described.

11) ENERGY BALANCE CONSTRAINTS

$$\begin{aligned} &P^{\mathrm{IES}}_{w,t} + P^{\mathrm{WG}}_{w,t} + P^{\mathrm{PVT}}_{w,t} + P^{\mathrm{CHP}}_{w,t} + P^{\mathrm{Ed}}_{w,t} \\ &\quad = P^{\mathrm{P2G}}_{w,t} + P^{\mathrm{EB}}_{w,t} + P^{\mathrm{Ec}}_{w,t} + PD^{e}_{w,t} + P^{\mathrm{EV}}_{w,t} \end{aligned} \tag{55}$$

$$\begin{aligned} &Q^{\mathrm{IES}}_{w,t} + Q^{\mathrm{WG}}_{w,t} + Q^{\mathrm{PVT}}_{w,t} \\ &\quad = QD^{e}_{w,t} \end{aligned} \tag{56}$$

$$\begin{aligned} &g^{\mathrm{IES}}_{w,t} + g^{\mathrm{P2G}}_{w,t} + g^{\mathrm{gas}}_{w,t} + g^{\mathrm{Gd}}_{w,t} \\ &\quad = g^{\mathrm{GB}}_{w,t} + g^{\mathrm{CHP}}_{w,t} + g^{\mathrm{Gc}}_{w,t} + gD^{g}_{w,t} \end{aligned} \tag{57}$$

$$\begin{aligned} &h^{\mathrm{CHP}}_{w,t} + h^{\mathrm{GB}}_{w,t} + h^{\mathrm{EB}}_{w,t} + h^{\mathrm{PVT}}_{w,t} + h^{\mathrm{Hd}}_{w,t} \\ &\quad = Q^{\mathrm{HR}}_{w,t} + h^{\mathrm{Hc}}_{w,t} + hD^{h}_{w,t} \end{aligned} \tag{58}$$

$$g^{bio}_{w,t} = g^{\mathrm{B2G}}_{w,t} \tag{59}$$

(55)-(59) demonstrate IEH energy balance of five types: electrical active power, electrical reactive power, natural gas, heat, and biogas. The left side of these equations is energy input, and the right side is output. Obviously, these energy balances need to be true at all moments. Through the conversion of electricity-heat, electricity-gas, heat-gas, biogas-gas, and biogas-heat, the complementary supply of electricity, heat, and gas is well realized.

B. ACTIVE DISTRIBUTION NETWORK MODELING

the SIES proposed in this paper involves ADN with two active management methods including reactive power compensation and demand response. Related constraints are exhibited separately as follow:

1) ACTIVE MANAGEMENT CONSTRAINTS

$$\begin{aligned} 0 \le Q^{\mathrm{SVC}}_{j,t} &\le \sum_{k} N^{\mathrm{SVC}}_{j,k} \bar{Q}^{\mathrm{SVC}}_{j,t} \\ j &\in \Theta_{\mathrm{SVC}}, \quad k \in \Omega_{\mathrm{SVC}}, \ \forall t \end{aligned} \tag{60}$$

$$PD^{e}_{j,t} = (1-\beta^{e}_{j,t}) \cdot \tilde{P}\tilde{D}^{e}_{j,t} \tag{61}$$

$$QD^{e}_{j,t} = (1-\beta^{e}_{j,t}) \cdot \tilde{Q}\tilde{D}^{e}_{j,t} \tag{62}$$

$$\begin{aligned} 0 \le \beta^{e}_{j,t} &\le \beta^{e}_{\max} \\ j &\in \Theta_{\mathrm{Bus}}, \quad \forall t \end{aligned} \tag{63}$$

In (60), the reactive power compensation range of SVC is stinted. And active and reactive power are curtailed with the same ratio, modelled in (61)-(63). To add, $\beta^{e}_{\max}$ shouldn't be greater than 1.

2) POWER FLOW CONSTRAINTS

$$\begin{aligned} \sum_{jk} P_{jk,t} = &\sum_{ij} P_{ij,t} - \sum_{ij} \hat{I}_{ij,t} \mathrm{R}_{ij} \\ &- P^{\mathrm{IES}}_{t,\mathrm{if}\{j\in\Theta_{\mathrm{IES}}\}} - PD^{e}_{t,\mathrm{if}\{j\in\Theta_{\mathrm{Bus}}\}} + P^{\mathrm{gen}}_{t,\mathrm{if}\{j\in\Theta_{\mathrm{gen}}\}} \end{aligned} \tag{64}$$

$$\begin{aligned} \sum_{jk} Q_{jk,t} = &\sum_{ij} Q_{ij,t} - \sum_{ij} \hat{I}_{ij,t} \mathrm{X}_{ij} - Q^{\mathrm{IES}}_{t,\mathrm{if}\{j\in\Theta_{\mathrm{IES}}\}} \\ &- QD^{e}_{t,\mathrm{if}\{j\in\Theta_{\mathrm{Bus}}\}} + Q^{\mathrm{gen}}_{t,\mathrm{if}\{j\in\Theta_{\mathrm{gen}}\}} + Q^{\mathrm{SVC}}_{t,\mathrm{if}\{j\in\Theta_{\mathrm{SVC}}\}} \end{aligned} \tag{65}$$

$$\hat{U}_{j,t} = \hat{U}_{i,t} - 2\left(P_{ij,t}\mathrm{R}_{ij} + Q_{ij,t}\mathrm{X}_{ij}\right) + \hat{I}_{ij,t}\left(\mathrm{R}^2_{ij} + \mathrm{X}^2_{ij}\right) \tag{66}$$

$$\begin{aligned} \hat{U}_{j,t}\hat{I}_{jk,t} &= P^2_{jk,t} + Q^2_{jk,t} \\ jk &\in \Theta^{\mathrm{from}}_{\mathrm{Brch}}, \quad ij \in \Theta^{\mathrm{to}}_{\mathrm{Brch}}, \ j \in \Theta_{\mathrm{Bus}}, \ \forall t \end{aligned} \tag{67}$$

where, the square terms of current and voltage are expressed as $\hat{I}_{j,t}$ and $\hat{U}_{j,t}$ to facilitate the solution. Subscript if$\{j \in \Theta\}$ in (64)-(65) is valid only when the bus j belongs to the set Θ, and $\Theta^{\mathrm{from}}_{\mathrm{Brch}}/\Theta^{\mathrm{to}}_{\mathrm{Brch}}$ denote the first/last nodes set of feeders.

3) SECURITY CONSTRAINTS

$$0 \le P_{ij} \le \sum_{k} \chi^{\mathrm{L}}_{ij,k} \bar{P}^{\mathrm{line}}_{k} \tag{68}$$

$$0 \le Q_{ij} \le \sum_{k} \chi^{\mathrm{L}}_{ij,k} \bar{Q}^{\mathrm{line}}_{ij} \tag{69}$$

$$\sum_{k} \chi^{\mathrm{L}}_{ij,k} = 1 \tag{70}$$

$$\underline{\hat{U}} \le \hat{U}_{j} \le \bar{\hat{U}} \tag{71}$$

$$\underline{P}^{\mathrm{gen}} \le P^{\mathrm{gen}}_{j} \le \bar{P}^{\mathrm{gen}} \tag{72}$$

$$\underline{Q}^{\mathrm{gen}} \le Q^{\mathrm{gen}}_{j} \le \bar{Q}^{\mathrm{gen}} \tag{73}$$

$$\chi^{\mathrm{L}}_{ij} \in \{0,1\}, \quad j \in \Theta_{\mathrm{Bus}}, \ ij \in \Theta_{\mathrm{Brch}}$$

In (68)-(70), the upper power flow limit of feeders is determined by upgrade situation, χ^{L}_{k} is the binary variable for that. (71) defines voltage safety range. And upper-level grid power supply restrictions are shown in (72)-(73).

VI. THE OPTIMAL MODELLING OF SIES AND IT'S LINEARIZATION METHOD

A. MODEL SUMMARY

Through the analysis of the components in section III-V, this paper proposes the optimal planning model of SIES, which will be introduced in detail below.

1) OBJECTIVE FUNCTION

This model aims to minimize the annual comprehensive cost, including investment costs and operating costs.

$$\min F = \mathbf{a} \cdot f_{\mathrm{inv}} + f^{\mathrm{ADN}}_{\mathrm{ope}} + f^{\mathrm{IEH}}_{\mathrm{ope}} + f^{\mathrm{Tr}}_{\mathrm{ope}} \tag{74}$$

a: INVESTMENT COSTS f_{inv}

$$\begin{aligned} f_{\mathrm{inv}} = &\sum_{\vartheta} \sum_{k\in\Omega_{\vartheta}} c^{\vartheta}_{k} N^{\vartheta}_{w,k} + \sum_{ij\in\Theta_{\mathrm{Brch}}} \sum_{k\in\Omega_{\mathrm{line}}} c^{\mathrm{L}}_{k} \chi^{\mathrm{L}}_{ij,k} \\ \vartheta \in &\{\Theta_{\mathrm{SVC}}, \Theta_{\mathrm{bio}}, \Theta_{\mathrm{WG}}, \Theta_{\mathrm{PVT}}, \Theta_{\mathrm{P2G}}, \Theta_{\mathrm{CHP}}, \\ &\Theta_{\mathrm{GB}}, \Theta_{\mathrm{FCF}}, \Theta_{\mathrm{B2G}}, \Theta_{\mathrm{ES}}, \Theta_{\mathrm{GS}}, \Theta_{\mathrm{HS}}\} \end{aligned} \tag{75}$$

b: THE OPERATING COSTS OF ADN f^{ADN}_{ope}

$$f^{\mathrm{ADN}}_{\mathrm{ope}} = f^{\mathrm{ADN}}_{\mathrm{enE}} + f^{\mathrm{ADN}}_{\mathrm{loss}} + f^{\mathrm{ADN}}_{\mathrm{cur\_load}} \tag{76}$$

$$f^{\mathrm{ADN}}_{\mathrm{enE}} = \sum_{t} \sum_{j\in\Theta_{\mathrm{gen}}} c^{\mathrm{enE}} P^{\mathrm{gen}}_{j,t} \tag{77}$$

$$f_{\text{loss}}^{\text{ADN}} = \sum_{t} \sum_{ij \in \Theta_{\text{Brch}}} c^{\text{loss}} \hat{I}_{ij,t} \text{R}_{ij} \tag{78}$$

$$f_{\text{cur\_load}}^{\text{ADN}} = \sum_{t} \sum_{j \in \Theta_{\text{Bus}}} c^{\text{cur\_load}} \beta_{j,t}^{e} \tilde{P} \tilde{D}_{j,t}^{e} \tag{79}$$

c: THE OPERATING COSTS OF IEH f_{ope}^{IEH}

$$f_{\text{ope}}^{\text{IEH}} = f_{\text{ope}}^{\text{cur\_DG}} + f_{\text{ope}}^{\text{DG}} + f_{\text{ope}}^{\text{P2G}} + f_{\text{ope}}^{\text{CHP}} + f_{\text{ope}}^{\text{GB}} + f_{\text{ope}}^{\text{EB}} + f_{\text{ope}}^{\text{B2G}} \tag{80}$$

$$f_{\text{ope}}^{\text{cur\_DG}} = \sum_{t} \sum_{w \in \Theta_{\text{IEH}}} c_{\text{P}}^{\text{cur\_DG}} \left[\left(\widehat{P}_{w,t}^{\text{WG}} - P_{w,t}^{\text{WG}} \right) + \left(\widehat{P}_{w,t}^{\text{PVT}} - P_{w,t}^{\text{PVT}} \right) \right] \tag{81}$$

$$f_{\text{ope}}^{\text{DG}} = \sum_{t} \sum_{w \in \Theta_{\text{IEH}}} \left[c_{\text{P}}^{\text{DG}} \left(P_{w,t}^{\text{WG}} + P_{w,t}^{\text{PVT}} \right) + c_{\text{h}}^{\text{PVT}} h_{w,t}^{\text{PVT}} \right] \tag{82}$$

$$f_{\text{ope}}^{\text{P2G}} = \sum_{t} \sum_{w \in \Theta_{\text{IEH}}} c^{\text{P2G}} P_{w,t}^{\text{P2G}} \tag{83}$$

$$f_{\text{ope}}^{\text{CHP}} = \sum_{t} \sum_{w \in \Theta_{\text{IEH}}} c^{\text{CHP}} g_{w,t}^{\text{CHP}} \tag{84}$$

$$f_{\text{ope}}^{\text{GB}} = \sum_{t} \sum_{w \in \Theta_{\text{IEH}}} c^{\text{GB}} g_{w,t}^{\text{GB}} \tag{85}$$

$$f_{\text{ope}}^{\text{EB}} = \sum_{t} \sum_{w \in \Theta_{\text{IEH}}} c^{\text{EB}} g_{w,t}^{\text{EB}} \tag{86}$$

$$f_{\text{ope}}^{\text{B2G}} = \sum_{t} \sum_{w \in \Theta_{\text{IEH}}} c^{\text{B2G}} g_{w,t}^{\text{B2G}} \tag{87}$$

d: THE OPERATING COSTS OF TN f_{ope}^{TN}

$$f_{\text{ope}}^{\text{TN}} = \sum_{t} \sum_{\forall [o,d]} \varsigma \left(f d_{od,t}^{\text{CV}} T_{od,t}^{\text{CV}} + f d_{od,t}^{\text{NV}} T_{od,t}^{\text{NV}} \right) \tag{88}$$

2) CONSTRAINS

The SIES model contains investment constrains and operation constrains of the ADN, the IEH, and the TN.

a: INVESTMENT CONSTRAINS Con-inv

$$0 \le \sum_{k} N_{w,k}^{\zeta} \le N_{\max}^{\zeta}, \quad \forall w \in \Theta_{\text{IEH}} \tag{89}$$

where superscript ζ represents all alternative equipment of SIES.

b: THE CONSTRAINS OF ADN Con − ADN

{(60)-(73)}

c: THE CONSTRAINS OF IEH Con − IEH

{(22)-(59)}

d: THE CONSTRAINS OF TN Con − TN

{(3)-(10), (13)-(21)}

B. LINEARIZATION METHODS

The proposed optimal model has several non-convex constraints, which is not convenient to solve the optimal value. Therefore, the linearization method of the nonlinear expression involved in this paper is introduced below.

1) MODIFIED PIECEWISE LINEARIZATION (MODIFIED PWL)

PWL is a method to analyze nonlinear system by dividing nonlinear function into several linear segments reasonably, whose effectiveness has been proven in [19]. In order to express the mathematical properties of original function, we usually take X points at equal intervals, corresponding horizontal coordinates are $x_i, i = 1, 2, \cdots, X$, and vertical ones are $y_i = f(x_i), i = 1, 2, \cdots, X$. However, only partial endpoint values are not a good representation of any value in the feasible region. Thus, SOS2 variable sets $\{m_i\}$ [26] are adopted in this paper as weight variables to approximate the target value.

Davidson function (8) is processed using the modified PWL, yielding:

$$\begin{cases} y_i^{\text{Davi}} = t_k^0 \cdot J_C \cdot \dfrac{x_i^{\text{Davi}}}{\bar{c}_k^0 - x_i^{\text{Davi}}} \\ x_{X^{\text{Davi}}}^{\text{Davi}} < \bar{c}_k^0 \\ f_{k,t}^{\text{CF}} = \sum_i m_i^{\text{Davi}} \cdot x_i^{\text{Davi}} \\ T_{k,t}^{\text{wait}} = \sum_i m_i^{\text{Davi}} \cdot y_i^{\text{Davi}} \\ \sum_i m_i^{\text{Davi}} = 1 \\ 0 \le m_i^{\text{Davi}} \le 1 \\ m_i^{\text{Davi}} \in \text{SOS2}, i = 1, 2, \cdots, X^{\text{Davi}} \end{cases} \tag{90}$$

In (90), the first equation is utilized to calculate endpoint value, and the third and fourth restate the original variables. What's more, it's noted that since the original function is meaningless at $x_i^{\text{Davi}} = \bar{c}_k^0$, the feasible range is slightly tightened as the second equation shown. The others are supplementary constraints on SOS2 set which are implemented by YALMIP toolbox expediently.

Similarly, deal with (18) and (22) and then get the relaxation expressions following:

$$\begin{cases} y_i^{\text{bio}} = a \left| x_i^{\text{bio}} - T_0^{\text{bio}} \right| + b \\ T^{\text{in}} = \sum_i m_i^{\text{bio}} \cdot x_i^{\text{bio}} \\ g^{\text{bio}} = \sum_i m_i^{\text{bio}} \cdot y_i^{\text{bio}} \\ \sum_i m_i^{\text{bio}} = 1 \\ 0 \le m_i^{\text{bio}} \le 1 \\ m_i^{\text{bio}} \in \text{SOS2}, i = 1, 2, \cdots, X^{\text{bio}} \end{cases} \tag{91}$$

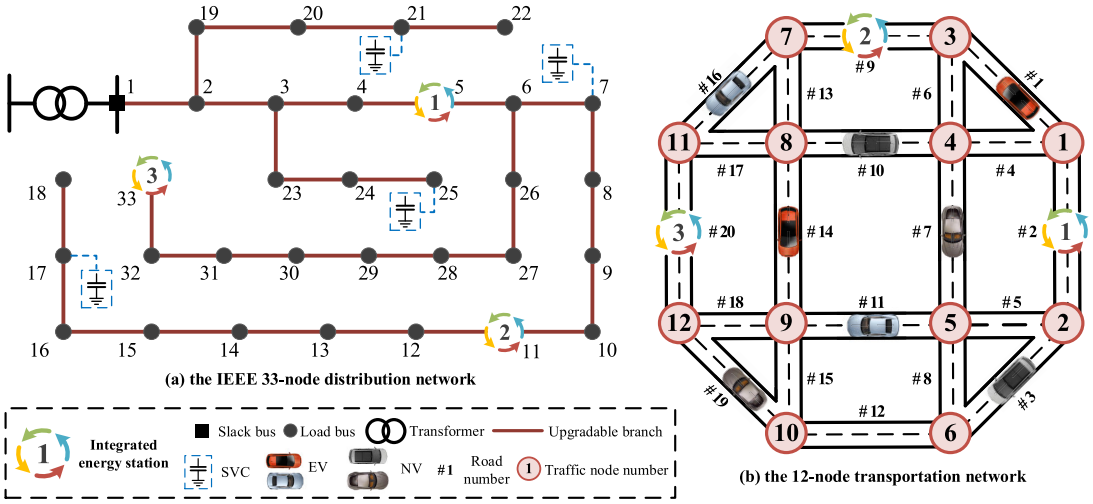

FIGURE 4. The topology diagram of SIES planning test case coupling ADN, TN, and IEH.

$$\begin{cases} y_i^{\mathrm{BPR}} = t_r^0 \left[1 + 0.15 \times \left(\dfrac{x_i^{\mathrm{BPR}}}{c_r^0} \right)^4 \right] \\ f_{r,t}^{\mathrm{road}} = \sum\limits_i m_i^{\mathrm{BPR}} \cdot x_i^{\mathrm{BPR}} \\ T_{r,t}^{\mathrm{BPR}} = \sum\limits_i m_i^{\mathrm{BPR}} \cdot y_i^{\mathrm{BPR}} \\ \sum\limits_i m_i^{\mathrm{BPR}} = 1 \\ 0 \le m_i^{\mathrm{BPR}} \le 1 \\ m_i^{\mathrm{BPR}} \in \mathrm{SOS2}, i = 1, 2, \cdots, X^{\mathrm{BPR}} \end{cases} \tag{92}$$

2) SECOND-ORDER CONE RELAXATION (SOCR) [27]

In line with [28], (67) is relaxed from the non-convex form to the following second-order cone form:

$$\left\| \begin{matrix} 2P_{jk,t} \\ 2Q_{jk,t} \\ \hat{I}_{jk,t} - \hat{U}_{j,t} \end{matrix} \right\|_2 \le \hat{I}_{jk,t} + \hat{U}_{j,t} \tag{93}$$

So far, the SIES planning model has been turned into mix-integrated second-order cone problem (MISOCP). The final model can be summarized as follows:

$$\begin{aligned} &\min\ F^{\mathrm{SIES}}:\ (74) \sim (88) \\ &s.t.\ \text{Con-inv':}\ (89) \\ &\quad \text{Con-ADN':}\ (60) \sim (66), (93), (68) \sim (73) \\ &\quad \text{Con-IEH':}\ (92), (23) \sim (59) \\ &\quad \text{Con-TN':}\ (3) \sim (7), (90), (9) \sim (10), \\ &\qquad\qquad (13) \sim (17), (91), (19) \sim (21) \end{aligned}$$

VII. CASE STUDY

A. BASIC PARAMETER SETTING

In this section, the IEEE 33-node distributed network [29] and a 12-node traffic network [30] are employed to verify the advantages of proposed model, whose topologies are shown in Fig.4. Two originally independent networks are coupled by three IEHs located in Buses No.5, No.11, No.33 of the ADN and Lines 1-2, 3-7, 11-12 of the TN respectively.

More detail parameters of SIES used in this paper's cases are as follow:

1) Most information of ADN is consistent with the standard one except power demand, which is exaggerated to 1.5 times in line with the development tendency of society. And considering the operating safety, the allowable voltage fluctuation range is 0.96-1.04. WG and PVT power factors are set to $\theta_{\max}^{\mathrm{WG}} = \theta_{\max}^{\mathrm{PVT}} = 0.9$, and the max curtailment percent of them is $\beta_{\max}^{\mathrm{WG}} = \beta_{\max}^{\mathrm{PVT}} = 50\%$.
2) Table 4 lists the maximum traffic demands of each O-D pair including EV demands and NV demands. And the basic traffic flow value is set to 20 vehicles/hour matching the system scale. Conversion parameter from traffic flow to charging demand is set as $\upsilon_{\mathrm{Tr}} = 0.5\mathrm{MW}$. Time shape coefficient J_C is assumed as 0.6.
3) The heat and gas demand around each IEH are summarized in Table 5. What's more, the table also displays the charging road capacity $\bar{c}_k^0$ in each IEH.
4) All alternative equipment information in this planning is shown in Table 6-11. For summary, device types include upgradable lines, SVCs, WGs, PVTs, BDs, P2Gs, CHPs, GBs, EBs, ESs, GSs, HSs and FCFs.
5) Table 12 summarizes the unit operating economic cost of each equipment involved, which is essential to the objective function of planning model.
6) The robust output sequences of renewable energy are extracted from the actual historical records, which are: DG output data, electric/gas/heat demand data from Elia Group in 2018 [31], traffic demand in 2019 [32] and temperature information in Beijing in 2018 [33].

TABLE 1. The planning results of the SIES model proposed in this paper.

	Items	Types	Planning results	Items	Types	Planning results
ADN	Upgraded line	I	5-6, 3-23, 6-26, 26-27, 32-33	SVC	I	-
		II	1-2, 2-3, 3-4, 4-5		II	7(2), 17(1), 25(2)
IEH	WG	I	#1(3), #2(4), #3(9)	EB	I	#2(1), #3(1)
		II	#2(1)		II	#1(1), #3(1)
	PVT	I	#1(2)	ES	I	#1(1), #2(1)
		II	#2(1), #3(1)		II	-
	P2G	I	-	GS	I	#2(1)
		II	#2(2), #3(3)		II	#3(1)
	CHP	I	#1(1), #2(1)	HS	I	#1(2), #2(1), #3(2)
		II	#3(1)		II	-
	GB	I	#1(1), #2(1)	FCF	I	#1(5), #2(5), #3(4)
		II	#3(1)		II	#1(5), #2(5), #3(4)
	BD	I	#1(1), #2(1), #3(1)	B2G	I	#1(1), #2(1), #3(1)

Notes: The number in ( ) indicates the number, and the position outside ( )

The representative scenarios are shown in Fig.12 and Fig.13 which reflect the volatility of renewable generations and various loads.

All simulations are completed on a personal computer. The mathematical modeling is programmed in MATLAB R2020a using YALMIP toolbox [34] and solved by GUROBI 9.0 [35].

B. PLANNING RESULTS AND ANALYSIS

For the convenience of subsequent analysis, the SIES planning model proposed in this paper is defined as **Case A**. The planning results calculated in 13379s are shown in Table 1, and the investment costs are shown in Table 2. According to the results, line upgrading mainly occurs around the main lines of the ADN and IEHs, which are both SIES power nodes. The DG supplies are mainly constructed in the IEH #3 with high energy demand, and the corresponding energy conversion devices are also configured with varying degrees of increase, not only to meet the energy demand of various forms, but also to use energy conversion to enhance the absorption efficiency of renewable energy. For the IEH #1 with no gas load, P2G devices are not equipped, but there is an increase in the number of energy conversion devices used to turn biogas into other energy forms. In addition, regardless of whether there are gas demands around the IEHs, each energy station chooses to build BDs, which highlights the green and economic advantage of biogas production, further proving that the biogas digesters play an indispensable role in the SIES. We also note that each IEH builds the same number of different types of FCFs, which is an intuitive expression of FCS-UE.

TABLE 2. The investment costs of the SIES model (10^4).

$f_{\mathbf{inv}}$	$f_{\mathrm{ope}}^{\mathrm{ADN}}$	$f_{\mathrm{ope}}^{\mathrm{IEH}}$	$f_{\mathrm{ope}}^{\mathrm{TN}}$	total cost F
1003.2	445.44	989.52	1176.2	2774.5

FCS-UE accurately represents the users' charging behavior. Fig.5 demonstrates the charging flow distribution in IEH #2 under FCS-UE. We find that when there are few CVs in the FCS, the vehicles always choose FCFs with the least comprehensive charging cost and charging time. This often happens at midnight and early morning, such as during the period in Fig. 5 where the queuing time is at an extremely low level; and when charging flow is heavy, EV users are shunted to another type of FCFs for charging, but the number of users who choose the FCFs with high fixed cost is always less than low. According to the analysis above, it's predictable that the queuing time surges if CV users always choose single type of FCF. Thus, two cases are designed to verify the utility of FCS-UE and mixed user equalization proposed in this paper.

Case B: No traffic information for charging flow at FCSs. All CV users choose the FCFs with lower fixed cost because of self-interest.

Case C: No road congestion information is available to EV users. All EV users select the shortest route to travel without changing their travel plans due to road congestion.

Comparing the results of Cases A, B, and C shown in Table 3 and Fig.6, conclusions are summarized below:

1) The total cost is greatly reduced under the FCS-UE pattern, especially for CV users. Fig. 6 demonstrates FCSs equivalent time cost of each IEH. The costs of Case A

TABLE 3. The planning results of FCSs in three comparative cases.

	Item	Case A	Case B	Case C
investment	FCF I	#1(5), #2(5), #3(4)	#1(8), #2(8), #3(8)	#1(8), #2(9), #3(7)
	FCF II	#1(5), #2(5), #3(4)	-	-
cost ($\$10^4$)	investment cost	36.775	35.969	35.966
	total cost-CV	181.50	189.72	190.39
	total cost-NV	994.75	994.81	995.56
	total cost	1213	1220.5	1221.9

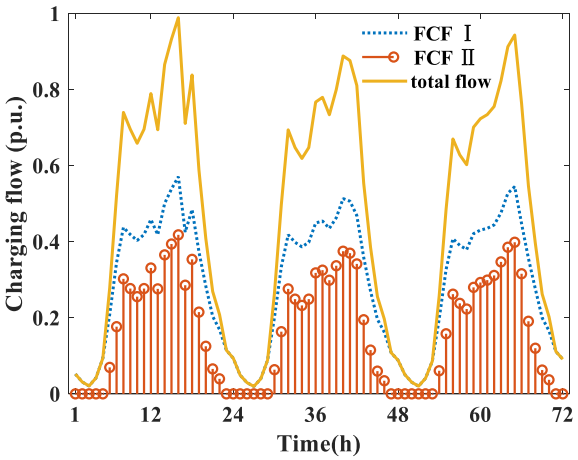

FIGURE 5. The charging flow distribution in IEH #2 under FCS-UE.

are significantly less than without and controlled below 50 minutes in all scenarios. Especially in the peak period of charging flow, such as 16:00 every day, the cost spike is most obviously reduced. Compared with ignoring CV charging guidance in FCSs (Case B), the maximum decrease is 15.98%; and with no EV traffic guidance in TN (Case C), 19.58% is the biggest drop. More intuitively, the total cost of CV is decreased by 4.67% compared by Case C. In addition, with the current proportion of CV, FCS-UE has little effect on NV analyzed by the similar cost of NV traveling.

2) Considering FCS-UE only increases the investment of FCFs slightly. FCSs average utilization rate is defined as $\left[\sum_w \sum_t (P^{EV}_{w,t} / \sum_k N^{CF}_{w,k} \bar{P}^{CF}_k)\right]/3$, and the results are 43.93% in Case A, 44.72% in Case B, and 44.70% in Case C. It can be concluded that diversion behavior under FCS-UE reduces average utilization of FCSs slightly, but these measures increase the diversity of users' choices.

Next, analyze the coupling relationship of various energies in IEHs of the SIES. Taking the planning and operation results under Case A as a reference, the transmission of each energy flow in IEH#2 is shown in Fig. 7, where the upper part of the abscissa axis is energy production, and the lower part is energy consumption. Comprehensive analysis of the conversion of three different energy forms (electricity, heat, and gas), the conclusions are as follows:

1) The outputs of BD and WG have good seasonal complementary characteristics. Due to the low wind resources in summer, WG outputs are at a low level throughout the year (orange color blocks in subgraph (a) of Fig. 7), while higher temperatures in summer are more suitable for fermentation of biogas digesters (yellow color blocks in subgraph (c) of Fig. 7). The situation is reversed in winter. At this time, wind resources are abundant, which just makes up for the energy gap caused by insufficient gas production due to low temperature. As a result of this complementarity, the direction of energy conversion varies in different seasons. In summer, gas energy is supplemented by electricity through the cogeneration device; in winter, electricity is mainly supplied to the gas load through

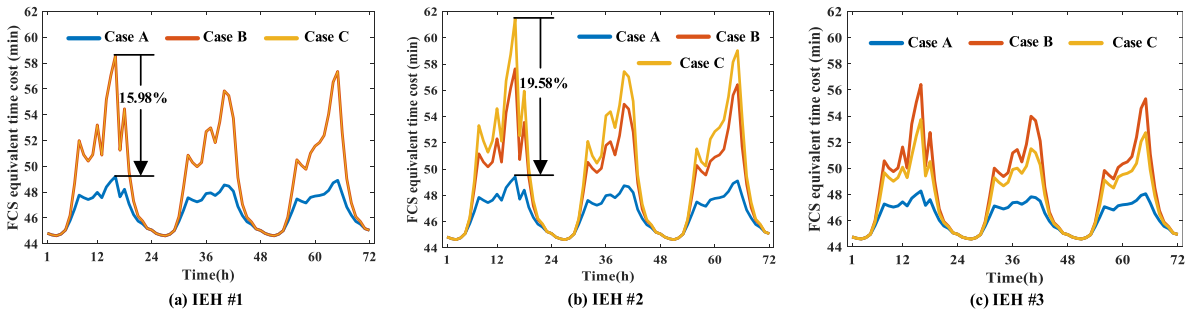

FIGURE 6. The FCSs equivalent time cost of each IEH.

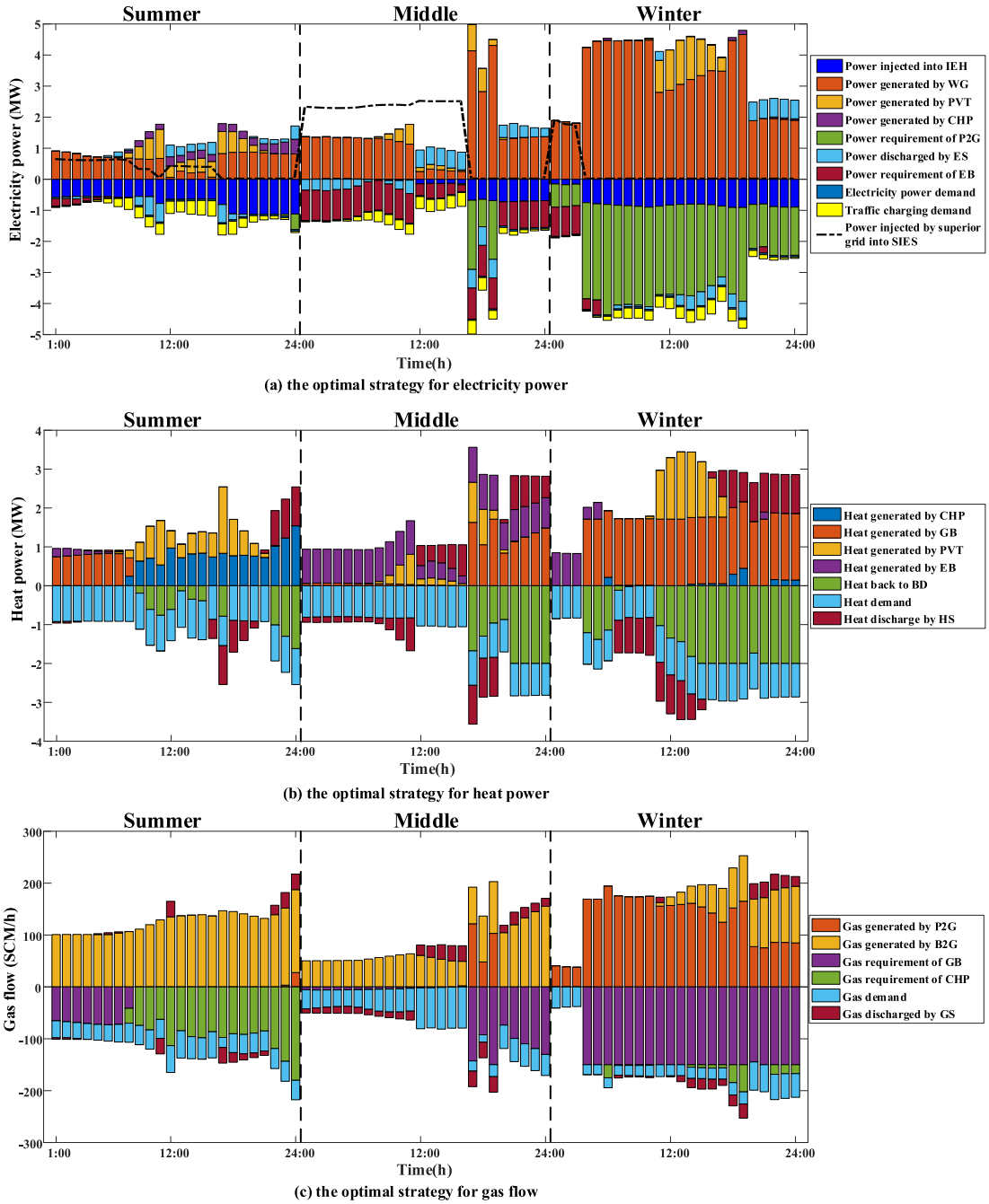

FIGURE 7. The optimal operation strategies for each energy flow in IEH#2.

P2Gs. In addition, the source of heat load supply also changes with the seasons, that is, from air to heat in summer using CHPs mainly, and from electricity to gas and then converted into heat in winter with P2Gs and GBs mainly.

2) The BD with heat feedback provides a new absorption channel for renewable energy. Its utility is most obvious in winter when WGs have high output. Surplus electricity is converted into gas through P2Gs, and then converted into heat energy through GBs to supply heat load, and the remainder is fed back to BDs to increase the fermentation temperature, thereby assisting gas production. On the other hand, SIES is 100% powered by renewable energy from 4:00 to 24:00 in winter, which shows that the system proposed in this paper can adapt to the access of high proportion of renewable energy.

In view of the above analysis, it's predicted that BDs with thermal feedback play an important role in the SIES. The working conditions of the BD are shown in Fig. 8, which

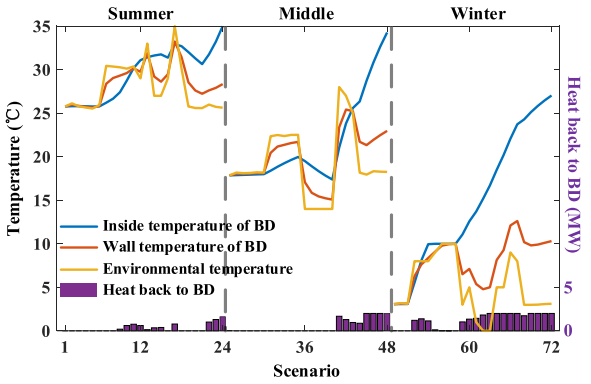

FIGURE 8. The working conditions of BD in different seasons.

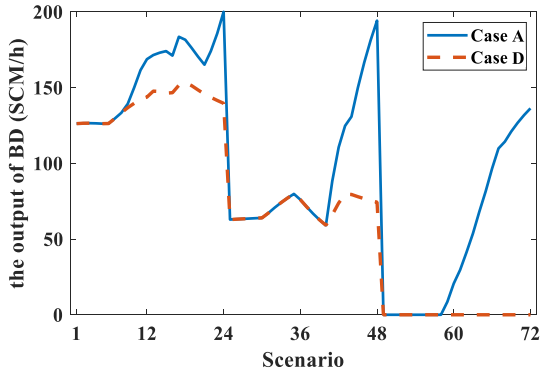

FIGURE 9. The working conditions of BD in Case A and D.

shows that the thermal feedback can effectively maintain the temperature insides at a certain level even in low temperature conditions (winter especially). And then, two cases are designed to further explore the important role of the BD model applied in this paper.

TABLE 4. The information of traffic demand (in p.u.).

Number	Origin	Destination	fd_{od}^{NV}	fd_{od}^{CV}
1	1	6	5	0
2	1	10	6	0.32
3	1	12	6	0.29
4	3	6	7	0
5	3	10	7	0.3
6	3	12	6	0.35
7	4	9	6	0
8	4	10	7	0.3
9	4	12	5	0.2

Case D: SIES planning choose the BD without thermal feedback mechanism, that is, only the room temperature determines the temperature of BD insides.

Case E: BD isn't the optional devices for SIES planning. SIES relies on the upper-level grid, WG, and PVT for energy supply.

Fig. 9 shows the output of BDs with and without thermal feedback. The results once again show that the feedback improves the gas supply capacity of traditional BDs, which is beneficial to suburbs with immature NGNs. In order to fully reflect well absorption capacity of BDs in this paper, Fig. 10 compares the consumption of WG and PVT of IEH #3

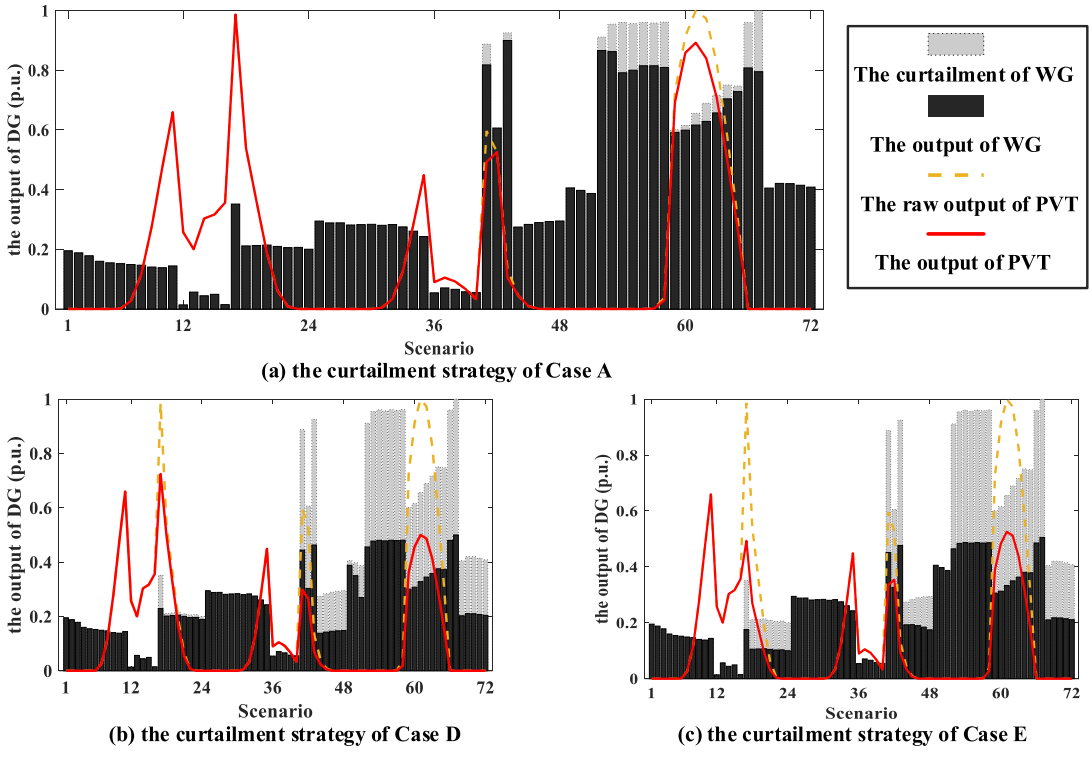

FIGURE 10. The curtailment strategy of Case A, Case D, and Case E.

TABLE 5. The information of IEH demand.

IEH number	ADN bus	TN road	Power demand/MW	Heat demand/MW	Gas demand/SCM	road capacity/p.u.
#1	5	1-2	0.09	1.68	0	1.5
#2	11	3-7	0.0675	1.07	90	1.5
#3	33	11-12	0.09	1.36	147.57	1.5

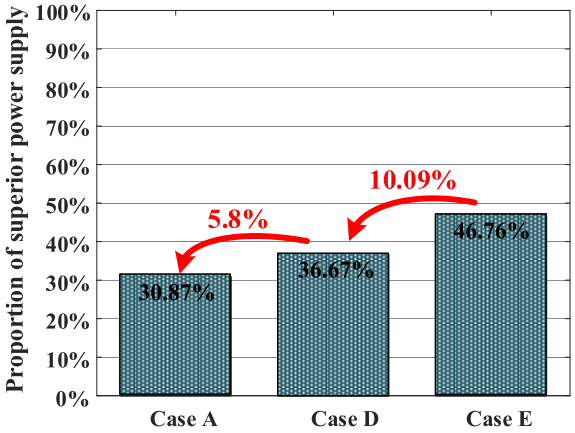

FIGURE 11. The Energy supply ratio of upper-level grid.

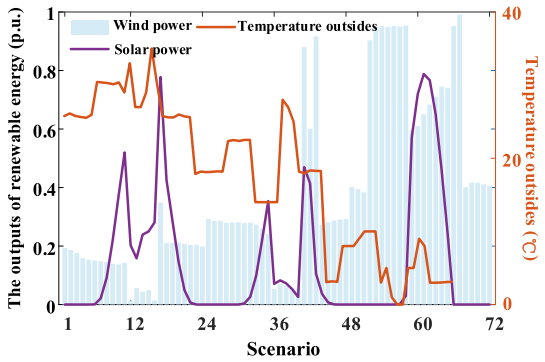

FIGURE 12. Wind power, solar power and temperature outsides in seasonal representative days.

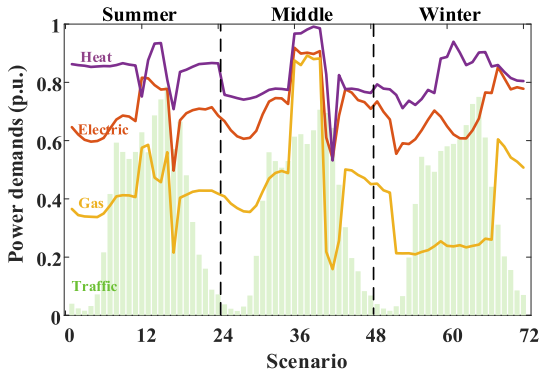

FIGURE 13. Electrical, heat, gas and traffic demand factors in seasonal representative days.

TABLE 6. The parameters of available power feeders.

Type	$\overline{P}_k^{\text{line}}$ (MW)	c_k^{L} ($)
original	0.6	0
I	1.4	158400
II	3	190200

TABLE 7. The parameters of available SVCs, WGs and PVTs.

Candidate device	Rated power	Investment cost ($)	Maximum quantity
SVC	0.04/0.08MVar	50000/80000	5
WG	0.8/1.5MW	105000/224000	12
PVT	1.0/1.8MW (electric) 1.2/2.2MW (heat)	102000/221000	12

in Cases A/D/E. It can be intuitively concluded that the model in this paper (the result shown in subgraph (a)) is good for the consumption of new energy devices, and only a few cases have the phenomenon of wind and light abandoning with less reduction, such as winter during the day; while no thermal feedback mechanism or ignoring BD investment greatly increases the reduction of renewable energy, especially in winter. The followings are quantitative analyses. According to statistics, the average reduction of WG for Cases A/D/E is 1.47%/8.1%/18.46% respectively, and those of PVT is 1.34%/4.14%/8.72%. Energy supply ratio of the upper-level grid is calculated by $\sum P_t^{\text{gen}} / \sum PD_t^{\text{e}}$, whose results are shown in Fig. 11. It's found that BD with thermal feedback reduces the dependence of SIES on the upper-level grid by 5.8% and 15.89% compared with Case D and Case E.

VIII. CONCLUSION

This article proposes a planning model for suburban integrated energy system. In this model, a new IEH that adapts to the weak current situation of suburban NGN and couples FCSs is developed. And a new mixed user equilibrium nesting FCS-UE is put forward to describe EV traveling behaviors. From the analysis of the simulation results, conclusions can be drawn as follows:

1) EV traveling behavior in line with new user equilibrium nesting FCS-UE decreases the cost greatly. In order to prove the superiority of the new equilibrium, two control groups are set, that is no CV charging guidance and no EV traffic guidance. The case studies show the maximum equivalent time reduction is up to 15.98% and 19.58%, respectively. What's more, CV users' cost is reduced under the FCS-UE mode proposed in this paper meanwhile considering the diversity of FCFs configurations.
2) BD with heat feedback has good renewable energy absorption capability. The outputs of BDs and WGs have seasonal complementary characteristics. Under this circumstance, the transfer of electricity-gas load between different seasons is realized by energy

TABLE 8. The parameters of available P2Gs, CHPs, GBs and EBs.

Candidate device	Efficiency	Rated power	Investment cost ($)	Maximum quantity
P2G	0.65	1/1.8MW	76500/102400	3
CHP	0.22 (gas to power)/ 0.72 (gas to heat)	180/280SCM	38100/52400	3
GB	0.96	150/240SCM	79500/112400	3
EB	0.9	1/2MW	68600/125000	3

TABLE 9. The parameters of available energy storage devices including ESs, GSs and HSs.

Candidate device	Efficiency	Rated power	Capacity	Investment cost ($)	Maximum quantity
ES	0.98	0.6/1.0MW	6/10MW	300000/500000	≤ DG quantities
GS	0.94	30/70SCM	130/400SCM	92900/191000	5
HS	0.98	1/2MW	8/16MW	91200/187000	5

TABLE 10. The parameters of available BD.

Fitting parameters	Insulation parameters	Attenuation parameters	Investment cost
$a=-8, b=200$	$C^{\text{in}}=0.52375\text{MWh}/^{\circ}\text{C}$ $C^{\text{W}}=0.1016\text{MWh}/^{\circ}\text{C}$	$R^{\text{in}}=9.051^{\circ}\text{C/MWh}$ $R^{\text{W}}=1.504^{\circ}\text{C/MWh}$ $R^{\text{out}}=3.517^{\circ}\text{C/MWh}$	$10000

TABLE 11. The parameters of available FCFs.

Type	Rated power (MW)	t_k^0 (min)	Charging cost($/kWh)	Investment cost ($)	Maximum quantity
I	0.06	12.5	0.1304	92050	16
II	0.045	16.67	0.1159	69300	16

TABLE 12. Unit operating economic cost of equipment involved.

Item	Cost	Item	Cost	Item	Cost
ς	2 $/min	$c_{\text{P}}^{\text{cur\_DG}}$	400 $/MWh	c^{CHP}	0.15 $/SCM
c^{enE}	140 $/MWh	c_{P}^{DG}	100 $/MW	c^{GB}	0.15 $/SCM
c^{loss}	140 $/MWh	$c_{\text{h}}^{\text{PVT}}$	50 $/MW	c^{EB}	100 $/MW
$c^{\text{cur\_load}}$	2000 $/MWh	c^{P2G}	100 $/MW	c^{B2G}	0.05 $/SCM

conversion devices. In addition, the thermal feedback mechanism can not only increase the annual biogas production of traditional BDs, but also provide a new channel for renewable energy consumption. Cases display that the annual abandonment of WG under this mechanism is only 1.47%, and of PVT is 1.34% merely. Furthermore, given that SIES has superior consumption ability, it's capable for SIES to operate under a high proportion of renewable energy access, and even the highest energy supply ratio can reach 100%.

However, the scope of this article is limited to the suburbs where the NGN is weak. With the continuous improvement of suburban supporting facilities, the NGN is bound to mature. Based on this trend, the study on expansion planning of SIES coupling ADN, TN, NGN, and suburban IEH is the next research direction of our team.

APPENDIX

See Figures 12 and 13, Tables 4–12.

REFERENCES

[1] *The Energy Progress Report, IEA, IRENA, UNSD, The World Bank*, World Health Organization, Geneva, Switzerland, 2020.

[2] J. Wu, J. Yan, H. Jia, N. Hatziargyriou, N. Djilali, and H. Sun, "Integrated Energy Systems," *Appl. Energy*, vol. 167, pp. 155–157, Apr. 2016. [Online]. Available: https://www.sciencedirect.com/science/article/pii/S0306261916302124?via%3Dihub

[3] D. Wang, L. Liu, H. Jia, W. Wang, Y. Zhi, Z. Meng, and B. Zhou, "Review of key problems related to integrated energy distribution systems," *CSEE J. Power Energy Syst.*, vol. 4, no. 2, pp. 130–145, Jun. 2018.

[4] State Grid. (2020). *New Infrastructure*. [Online]. Available: http://www.sgcc.com.cn/
[5] New Energy and Industrial Technology Development Organization. (2020). *Japan Smart Community Alliance*. [Online]. Available: https://www.nedo.go.jp/english/
[6] United States Department of Energy Office of Electric Transmission and Distribution. (2003). *Grid 2030*. [Online]. Available: https://www.energy.gov/sites/prod/files/oeprod/DocumentsandMedia/Electric_Vision_Document.pdf
[7] W. Huang, N. Zhang, J. Yang, Y. Wang, and C. Kang, "Optimal configuration planning of multi-energy systems considering distributed renewable energy," *IEEE Trans. Smart Grid*, vol. 10, no. 2, pp. 1452–1464, Mar. 2019.
[8] J. Wang, Z. Hu, and S. Xie, "Expansion planning model of multi-energy system with the integration of active distribution network," *Appl. Energy*, vol. 253, Nov. 2019, Art. no. 113517.
[9] Q. Zeng, B. Zhang, J. Fang, and Z. Chen, "A bi-level programming for multistage co-expansion planning of the integrated gas and electricity system," *Appl. Energy*, vol. 200, pp. 192–203, Aug. 2017.
[10] G. Pan, W. Gu, H. Qiu, Y. Lu, S. Zhou, and Z. Wu, "Bi-level mixed-integer planning for electricity-hydrogen integrated energy system considering levelized cost of hydrogen," *Appl. Energy*, vol. 270, Jul. 2020, Art. no. 115176.
[11] H. Fan, Q. Yuan, S. Xia, J. Lu, and Z. Li, "Optimally coordinated expansion planning of coupled electricity, heat and natural gas infrastructure for multi-energy system," *IEEE Access*, vol. 8, pp. 91139–91149, 2020.
[12] T. Sarkar, A. Bhattacharjee, H. Samanta, K. Bhattacharya, and H. Saha, "Optimal design and implementation of solar PV-wind-biogas-VRFB storage integrated smart hybrid microgrid for ensuring zero loss of power supply probability," *Energy Convers. Manage.*, vol. 191, pp. 102–118, Jul. 2019.
[13] B. Zhou, D. Xu, C. Li, C. Y. Chung, Y. Cao, K. W. Chan, and Q. Wu, "Optimal scheduling of biogas–solar–wind renewable portfolio for multicarrier energy supplies," *IEEE Trans. Power Syst.*, vol. 33, no. 6, pp. 6229–6239, Nov. 2018.
[14] D. Xu, B. Zhou, K. W. Chan, C. Li, Q. Wu, B. Chen, and S. Xia, "Distributed multienergy coordination of multimicrogrids with biogas-solar-wind renewables," *IEEE Trans. Ind. Informat.*, vol. 15, no. 6, pp. 3254–3266, Jun. 2019.
[15] D. Mao, J. Tan, and J. Wang, "Location planning of PEV fast charging station: An integrated approach under traffic and power grid requirements," *IEEE Trans. Intell. Transp. Syst.*, early access, Jun. 23, 2020, doi: 10.1109/TITS.2020.3001086.
[16] H. Hou, M. Xue, Y. Xu, Z. Xiao, X. Deng, T. Xu, P. Liu, and R. Cui, "Multi-objective economic dispatch of a microgrid considering electric vehicle and transferable load," *Appl. Energy*, vol. 262, Mar. 2020, Art. no. 114489.
[17] W. Wei, L. Wu, J. Wang, and S. Mei, "Network equilibrium of coupled transportation and power distribution systems," *IEEE Trans. Smart Grid*, vol. 9, no. 6, pp. 6764–6779, Nov. 2018.
[18] S. Xie, Z. Hu, J. Wang, and Y. Chen, "The optimal planning of smart multi-energy systems incorporating transportation, natural gas and active distribution networks," *Appl. Energy*, vol. 269, Jul. 2020, Art. no. 115006.
[19] S. Xie, Z. Hu, and J. Wang, "Scenario-based comprehensive expansion planning model for a coupled transportation and active distribution system," *Appl. Energy*, vol. 255, Dec. 2019, Art. no. 113782.
[20] F. Trespalacios and I. E. Grossmann, "Improved Big-M reformulation for generalized disjunctive programs," *Comput. Chem. Eng.*, vol. 76, pp. 98–103, May 2015.
[21] K. B. Davldson, "A flow travel time relationship for use in transportation planning," *Commissioner Main Roads*, vol. 3, pp. 183–194, Mar. 1978. [Online]. Available: https://www.researchgate.net/publication/280964779_A_flow-travel_time_relationship_for_use_in_transportation_planning
[22] J. G. Wardrop, "Some theoretical aspects of road traffic research," *OR, Oper. Res. Quart.*, vol. 4, pp. 72–73, Jan. 1953. [Online]. Available: https://www.researchgate.net/publication/245534689_Correspondence_Some_theoretical_aspects_of_road_traffic_research
[23] *Traffic Assignment Manual*, U.S. Dept. Commerce, Washington, DC, USA, 1964.
[24] V. C. Weatherford and Z. Zhai, "Affordable solar-assisted biogas digesters for cold climates: Experiment, model, verification and analysis," *Appl. Energy*, vol. 146, pp. 209–216, May 2015.
[25] M. M. Haghighi, "Controlling energy-efficient buildings in the context of smart grid: A cyber physical system approach," Tech. Rep., 2013. [Online]. Available: https://www2.eecs.berkeley.edu/Pubs/TechRpts/2013/EECS-2013-244.html
[26] E. M. L. Beale and J. A. Tomlin, "Special facilities in a general mathematical programming system for nonconvex problems using ordered sets of variables," *Oper. Res.*, vol. 69, pp. 447–454, Jan. 1969. [Online]. Available: https://www.researchgate.net/publication/313166553_Special_facilities_in_a_general_mathematical_programming_system_for_nonconvex_problems_using_ordered_sets_of_variables
[27] M. S. Lobo, L. Vandenberghe, S. Boyd, and H. Lebret, "Applications of second-order cone programming," *Linear Algebra Appl.*, vol. 284, nos. 1–3, pp. 193–228, Nov. 1998.
[28] M. Farivar and S. H. Low, "Branch flow model: Relaxations and convexification—Part I," *IEEE Trans. Power Syst.*, vol. 28, no. 3, pp. 2554–2564, Aug. 2013.
[29] M. E. Baran and F. F. Wu, "Network reconfiguration in distribution systems for loss reduction and load balancing," *IEEE Trans. Power Del.*, vol. 4, no. 2, pp. 1401–1407, Apr. 1989.
[30] W. Wei, L. Wu, J. Wang, and S. Mei, "Expansion planning of urban electrified transportation networks: A mixed-integer convex programming approach," *IEEE Trans. Transport. Electrific.*, vol. 3, no. 1, pp. 210–224, Mar. 2017.
[31] Elia Group. (2020). *Load Data*. [Online]. Available: https://www.elia.be/en/grid-data
[32] NREL Transforming Energy. *Traffic Data*. Accessed: Feb. 2020. [Online]. Available: https://www.nrel.gov/transportation/secure-transportation-data/tsdc-california-vehicle-survey-2017.html
[33] China Meteorological Administration. (2020). *Weather Data*. [Online]. Available: http://www.weather.com.cn/
[34] YALMIP. *Download*. Accessed: Oct. 2020. [Online]. Available: https://yalmip.github.io/
[35] Gurobi. *Gurobi Optimization*. Accessed: Oct. 2020. [Online]. Available: https://www.gurobi.com/

CHANGHONG WENG was born in Fuzhou, Fujian, China, in 1997. He received the B.S. degree from the School of Electrical Engineering and Automation, Fuzhou University, Fujian, in 2019. He is currently pursuing the M.S. degree with the School of Electrical Engineering and Automation, Wuhan University.

His research interest includes the planning methods and operating strategies of integrated energy systems.

ZHIJIAN HU (Member, IEEE) received the B.E. degree in electrical engineering from the Shanghai University of Electric Power, Shanghai, China, in 1991, and the M.E. and Ph.D. degrees in electrical engineering from the Wuhan University of Hydraulic and Electric Engineering, Wuhan, China, in 1996 and 1999, respectively. From 2006 to 2007, he was an Academic Visitor at the School of Electrical and Electronic Engineering, The University of Manchester, Manchester, U.K. He is currently a Professor with the School of Electrical Engineering and Automation, Wuhan University, Wuhan. His special fields of interest include power system dynamics and power system planning.

SHIWEI XIE received the B.S. degree from the School of Electrical Engineering and Automation, Fuzhou University, Fujian, China, in 2016. He is currently pursuing the Ph.D. degree with the School of Electrical Engineering and Automation, Wuhan University. His research interests include coupling planning of active distribution networks and traffic networks.

ZHI CHEN was born in Yibin, Sichuan, China, in 1997. She received the B.S. degree from the School of Electrical Engineering and Automation, Wuhan University, Hubei, China, in 2019, where she is currently pursuing the M.S. degree. Her research interests include the planning methods and operating strategies of the park-level integrated energy systems.

SHENGHUI LIU received the B.S. degree in electrical engineering from Northeastern University, in 2018. His research interests include applications of deep learning in power system analytics and operation.

YIXING DU received the B.S. degree in electrical engineering from Hunan University, Changsha, China, in 2019. He is currently pursuing the M.S. degree with the School of Electrical Engineering and Automation, Wuhan University, Wuhan, China. His research interests include transient stability assessment of power systems, data mining, and deep learning.